First measurement of direct photoproduction of the $a_2(1320)^0$ meson on the proton

g12

energy resolution $0.1\%E_0$ was used to tag photons in the energy range $0.2E_0$–$0.95E_0$ [12, 13]. The target was a 40-cm-long cell filled with LH_2. During the run, the high-intensity photon flux, $\approx 4 \times 10^7$ γ/s, was measured by sampling the "out-of-time" electron hits in the photon tagger [14].

Outgoing particles were measured with the CLAS detector [15]. This was a large-acceptance spectrometer, based on a toroidal magnet made of six superconducting coils arranged symmetrically around the beamline [16]. The momentum of a charged particle was determined from the radius of curvature of its trajectory in the magnetic field as measured by a multi-wire drift-chamber system (DC) [17]. A set of plastic scintillator counters (TOF), installed behind the drift chambers, provided the time of flight of each particle [18]. Particle identification was performed through the β vs. p technique. The energies and angles of the photons were measured with a lead/scintillator electromagnetic calorimeter (EC), covering polar angles in the range 8°–45°, with energy resolution $\sigma_E/E \approx 10\%/\sqrt{E(\mathrm{GeV})}$, and angular resolution $\sigma_\theta \approx 10$ mrad [19].

The incoming photon was identified based on a $\pm$ 1.0 ns coincidence between the vertex times obtained from the photon tagger and from the CLAS detector. The latter was determined by measuring the time of the outgoing charged particles with an array of plastic scintillator counters (ST) surrounding the target [20]. Due to the large photon flux, a fraction $f_{multi-\gamma} = 12.5\%$ of events with more than one tagged photon within the coincidence window was observed. To avoid any bias in the analysis, these events were discarded. This effect was accounted for in the cross-section normalization by scaling the measured event yield by $1/(1 - f_{multi-\gamma})$. The systematic uncertainty of this correction, evaluated from the run-by-run variation of $f_{multi-\gamma}$, is $\approx 0.7\%$.

The trigger condition required one charged particle and two photons in the CLAS detector. The corresponding efficiency was evaluated from minimum bias runs and found to be on average $\varepsilon_{\mathrm{trg}} = 80\%$. A trigger efficiency map was derived and used to correct the cross-section normalization for the residual efficiency dependence on the charged particle impact point on the detector.

This analysis focuses on the $\gamma p \to \pi^0 \eta p$ reaction, with all three final-state hadrons measured. Although CLAS was optimized for charged multi-particle final states, this reaction could be measured thanks to the high statistics and the specific setup of the g12 run, with the target moved upstream to maximize the detector acceptance. Events were selected requiring detection of both the proton and the four photons from the π^0 and η decay. The standard g12 procedures, including momentum corrections and fiducial cuts, were applied [21]. A $4C$ kinematic fit (energy and momentum conservation imposed) was used to select events belonging to the exclusive $\gamma p \to 4\gamma p$ reaction, by introducing a cut on the corresponding confidence level (CL) [22, 23]. To optimize this cut, the difference between the missing mass on the proton squared and the four photon invariant mass squared – here denoted as K – was considered. From energy and momentum conservation, it follows that signal events ($\gamma p \to 4\gamma p$) are distributed around $K = 0$ with a gaussian distribution, while background events ($\gamma p \to 4\gamma p X$) manifest as a tail in the $K > 0$ region. Therefore, the following figure of merit (FOM) was defined:

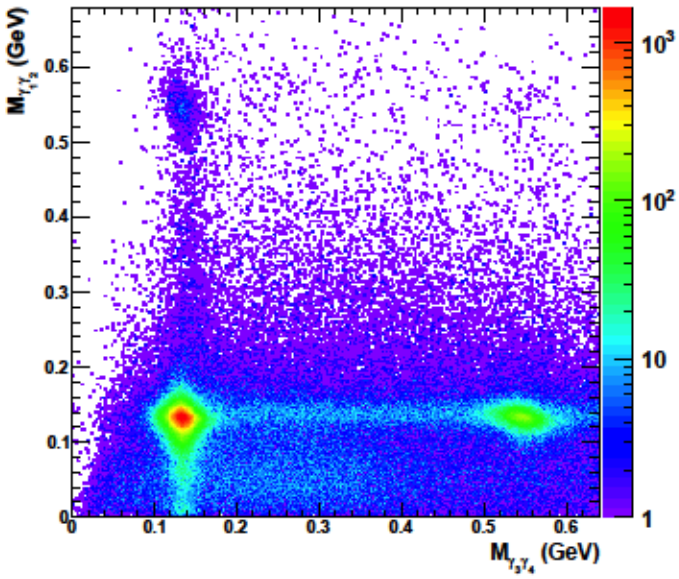

FIG. 1. Correlation between the invariant mass of the two photon pairs for exclusive $\gamma p \to 4\gamma p$ events. In each event, γ_1 and γ_2 are the photons with the smallest opening angle. The bottom-right cluster contains signal events from the $\gamma p \to \pi^0 \eta p$ reaction.

$$\mathrm{FOM} = \frac{n_s}{\sqrt{n_s + n_b}}\,, \tag{1}$$

where $n_s/2$ ($n_s/2 + n_b$) was the number of events with $K < 0$ ($K > 0$). The optimal CL cut was determined by maximizing the FOM, and found to be 1.86%.

The following procedure was then adopted to isolate the $\gamma p \to \pi^0 \eta p$ reaction. First, the photons were ordered event-by-event by naming γ_1 and γ_2 those with the smallest opening angle. This algorithm exploits the fact that, due to the lower π^0 mass, the two photons from its decay are expected to have, on average, a smaller opening angle than those from η decay. The corresponding efficiency, estimated from Monte Carlo simulations, is approximately 82% [24]. The correlation between the invariant masses of the two photon pairs, $M_{\gamma_1\gamma_2}$ vs. $M_{\gamma_3\gamma_4}$ is shown in Fig. 1. Signal events were identified as those corresponding to the bottom-right cluster centered at $M_{\gamma_1\gamma_2} = M_{\pi^0}, M_{\gamma_3\gamma_4} = M_\eta$. A small fraction of events, corresponding to $\approx 4\%$ of the main signal yield, appeared in the opposite combination, and was not considered in

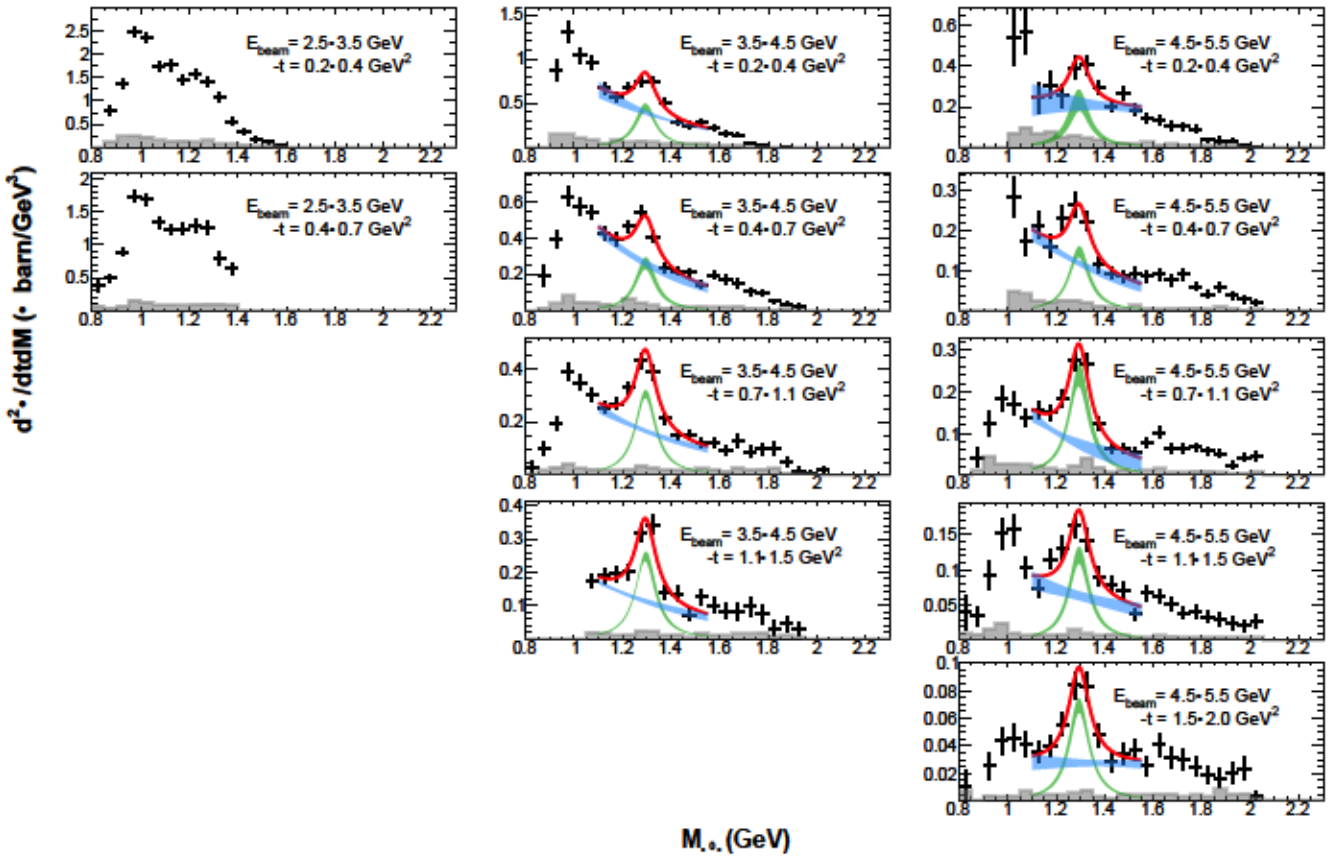

FIG. 2. Differential cross section for the reaction $\gamma p \to \pi^0 \eta p$. Each histogram reports the reaction differential cross section $d^2\sigma/dtdM$ as a function of the $\pi^0\,\eta$ invariant mass, for the specific E_{beam} and $-t$ bin reported in the same panel. The bottom gray-filled area in each panel shows the systematic uncertainty. The red curve is the result from the best fit performed with the model described in the text. The green and blue areas correspond, respectively, to the contribution of the a_2 resonance and of the background, here reported as the $\pm 1\sigma$ systematic uncertainty bands around the central value. *These have been scaled vertically by a factor* $\times 2$ *for better readability.*

while the width Γ_{a_2} was fixed to the nominal PDG value, (113.4 ± 1.3) MeV – the effect of this choice was studied and included in the systematic uncertainty. The χ^2/NDF value was $64.3/53 = 1.21$, and the obtained M_{a_2} value was (1308 ± 2) MeV, in very good agreement with the nominal PDG value, (1312.2 ± 2.8) MeV. The fit result is reported for each kinematic bin in Fig. 2 as a red curve, while the green (blue) areas shows the a_2 (background) contribution only, reported as the $\pm 1\sigma$ systematic uncertainty band around the central value.

The differential cross section for the reaction $\gamma p \to a_2(1320)^0\, p$ was finally obtained by integrating the resonance term in each kinematic bin, accounting for the $a_2 \to \pi^0\eta$ branching fraction, $(14.5 \pm 1.2)\%$ [26]. The results are shown in Fig. 3, where the black (red) points refer to the photon energy range 3.5–4.5 GeV (4.5–5.5 GeV). For each data point, the vertical bar shows the statistical uncertainty, evaluated from the covariance matrix of the χ^2 fit. The colored bands at the bottom show the systematic uncertainty, obtained summing quadratically the systematic uncertainty for $d^2\sigma/dtdM$ and that associated with the fit procedure. This was evaluated by repeating the fit with different choices of the fit range and of the a_2 width, that was varied within $\pm 2\sigma$ around the nominal value. M_{min} (M_{max}) was varied in the interval 1.0–1.1 GeV (1.55–1.7 GeV). The nominal range reported previously corresponds to the fit with the smallest χ^2/NDF value. The argument of the exponential function was also replaced by polynomials of various orders. The systematic uncertainty was calculated, in each bin, as the RMS of the cross-section values obtained from the different fits.

The most intriguing feature of the $\gamma p \to a_2(1320)\, p$ cross section is the presence of a dip at $-t_{dip} \approx 0.55\,\mathrm{GeV}^2$, observed simultaneously at both beam energies. The hypothesis that this observed was just the effect of a statistical fluctuation was excluded at 99% CL as follows. We made a null hypothesis for $d\sigma/dt$, assuming a monotone shape: we tested both a linear and an exponential behavior. In particular, for this $-t$ and E_{beam} range, within the precision dictated by the large

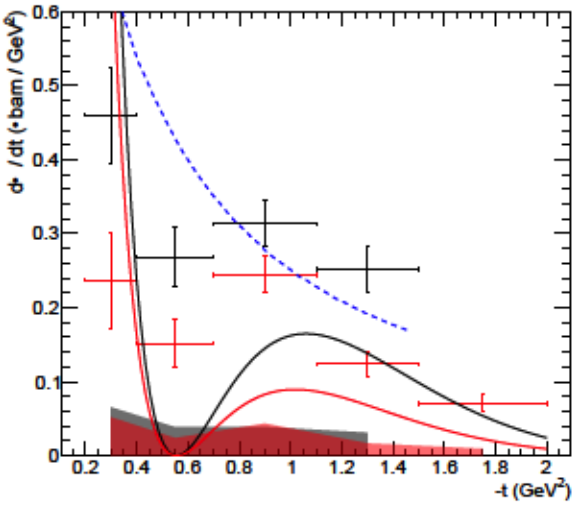

FIG. 3. Differential cross section $d\sigma/dt$ for the reaction $\gamma p \to a_2(1320)p$, for $E_{\text{beam}} = 3.5$–$4.5\,\text{GeV}$ (black) and $E_{\text{beam}} = 4.5$–$5.5\,\text{GeV}$ (red). The vertical error bars show the statistical uncertainty, whereas horizontal error bars correspond to the $-t$ bins width. The bottom bands show the systematic uncertainty. The continuous lines are predictions from the JPAC model [27], computed respectively for a beam energy of 4 GeV (black) and 5 GeV (red). The blue dashed line is the prediction from the model by Xie *et al.* [28], for beam energy 3.4 GeV. *For better readability, this was scaled vertically by a factor* $\times 0.5$.

statistical errors, the latter functional form should generally provide a sufficient description of $\frac{d\sigma}{dt}$ in the absence of a dip. We generated $N = 10^5$ toy Monte Carlo datasets, re-sampling each measured $d\sigma/dt$ point $y_t \pm \sigma_t$ from a Gaussian distribution with $\mu = y_t$ and $\sigma = \sigma_t$. Conservatively, we adopted for σ_t the quadratic sum of the statistical and systematic uncertainties, excluding the contributions that are indepedentent from the kinematic bin. For each toy dataset and each beam energy, we performed a fit with the hypothesized functional form, excluding the point in the dip, extrapolating from it the expected cross-section value at $-t_{dip}$. The bin width was taken into account by computing the latter as the average cross-section value inside the $-t_{dip}$ bin. Finally, from the fraction of toy datasets in which both extrapolated values were lower than the toy dataset values at $-t_{dip}$, we computed the null hypothesis $p-$value.

The origin of the dip and its specific location can be explained in the context of Regge theory [29]. In Fig. 3, we show the results of a model based on a Regge-theory production amplitude parametrization developed by the JPAC Collaboration [27], computed for the two beam energies 4 GeV (black) and 5 GeV (red). The amplitude includes the leading vector trajectories only, which have the ρ and ω quantum numbers. Regge-resonance duality implies that the parameters of Regge amplitudes corresponding to these vector exchanges are closely related to the ones involving the tensor a_2 and f_2 mesons (exchange degeneracy hypothesis [29, 30]). Since no scalar mesons lie on the a_2 trajectory, the residue of the tensor exchange has to vanish when the Regge trajectory $\alpha(t)$ is equal to zero to remove the scalar pole. Vector exchanges, which share the residues with the tensors, will thus also vanish at $\alpha(t) = 0$, that is at $-t = m^2_{\rho,\omega} \approx 0.55\,\text{GeV}^2$, leading to an exact zero in the cross section. However, subleading Regge poles or cut contributions can turn the zero of the amplitude into the dip observed in data and improve the description at higher $-t$. The results presented here are a pure prediction for $d\sigma/dt$, since the model parameters were tuned on different datasets: the qualitative agreement between data and model, in particular concerning the position of the dip, demonstrates the effectiveness of a reaction amplitude parametrization based on Regge phenomenology. The use of the present data to fine-tune the model parameters is beyond the scope of this work, and will be the subject of a different publication [27]. Finally, we observe that our new data will help in understanding the nature of the $a_2(1320)$ resonance. While many authors describe it as a $q\overline{q}$ state [31], others propose a different description. For example, Xie *et al.* [28] recently developed a model where the a_2 is a molecular state dynamically generated from the $\rho - \omega$ and $\rho - \phi$ interactions in S-wave with spin 2. This model predicts a smooth $d\sigma/dt$ shape, without any dip. Our data rules out this hypothesis.

In summary, we have measured for the first time the reaction $\gamma p \to \pi^0 \eta p$ in the photon beam energy range 3.5–5.5 GeV, and for four-momentum transferred squared values between 0.2 and $2.0\,\text{GeV}^2$, extracting the cross section for the exclusive $a_2(1320)$ photoproduction on the proton. The cross section shows a pronounced dip at $-t \approx 0.55\,\text{GeV}^2$, which can be explained in the framework of Regge theory. Since the $a_2(1320)^0$ is the most prominent structure present in the $\pi^0\eta$ invariant mass, detailed knowledge of its production cross section is valuable for any assessment of a possible exotic resonance contribution. This measurement will thus help high statistics photoproduction experiments, *e.g.* CLAS12 [32], GLUEX [33], and BGOOD [34], to better understand the $\pi^0\eta$ mass spectrum and to properly describe the production of the dominant a_2 resonance, using it as a benchmark in the search for exotic states.

This work was supported by: the U.S. Department of Energy (DOE), the U.S. National Science Foundation, the U.S. Jeffress Memorial Trust; the Physics and Astronomy Department and the Office of Research and Economic Development at Mississippi State University, the United Kingdom's Science and Technology Facilities Council (STFC), the Italian Istituto Nazionale di Fisica Nucleare; the French Institut National de Physique Nucléaire et de Physique des Particules, the French Centre National de la Recherche Scientifique; and the National Research Foundation of Korea. This material is

https://www.jlab.org/Hall-B/notes/clas_notes05/2005-002.pdf

---

*

†

‡

§

¶

g12

https://misportal.jlab.org/ul/Physics/Hall-B/clas/viewFile.cfm/2017-002.pdf?documentId=756

https://misportal.jlab.org/ul/Physics/Hall-B/clas/viewFile.cfm/2010-015.pdf?documentId=614

https://www.jlab.org/Hall-B/notes/clas_notes03/03-017.pdf